

# Theoretical Analysis of the Effects of Band Gaps and the Conduction Band Offset of ZnS-CIGS Layers, as Well as Defect Layer Thickness

Adama Sylla<sup>1</sup>, Siaka Touré<sup>2</sup>, Jean-Pierre Vilcot<sup>3</sup>

<sup>1,2</sup>Laboratoire d'Énergie Solaire, Université Félix Houphouët Boigny, 22 BP. 582, Abidjan 22 Cote d'Ivoire.

<sup>3</sup>Institut d'Électronique, de Microélectronique et de Nanotechnologie (IEMN), UMR, CNRS, 8520. Laboratoire Central, Cité Scientifique – Avenue Poincaré – BP 60069, 59652 Villeneuve d'Ascq Cedex, Lille1, France.

**Abstract:** This article deals with solar cells based on  $\text{CuIn}_x\text{Ga}_{1-x}\text{Se}_2$  (CIGS) without the toxic cadmium buffer. The software named AFORS-HET is used to simulate the solar cell,  $n\text{-ZnS}/p\text{-CIGS}$ , in the structure  $n\text{-ZnO}/\text{Al}/i\text{-ZnO}/n\text{-ZnS}/p\text{-CIGS}/\text{Mo}$ . The Ga-content of the  $\text{CuIn}_{1-x}\text{Ga}_x\text{Se}_2$  absorber is  $x = 0.31$  with an energy band gap of 1.19 eV. The optimum conversion efficiency achieved is found to be 26%. The simulation results have shown that the ZnS buffer layer band gap does not influence the solar cell performance. On the other hand, the cell characteristic parameters were found to be more sensitive to the CIGS layer band gap variation and conduction band offset. We also analyse the effects of the band gap and thickness of the defect layer on the solar cell performance. The optimum band gap and thickness were found to be equal to 1.25 eV and 15 nm respectively.

**Keywords:**  $\text{Cu}(\text{In}_{1-x}\text{Ga}_x)\text{Se}_2$ , thin-film solar cell, numerical simulation, AFORS-HET, band offset.

## 1. Introduction

In the structure of solar cells based on CIGS, the entire photo-generation of the carriers must take place within the CIGS absorber. The role of the ZnS buffer is to participate in the formation of the ordered defect compound (ODC)/CIGS homojunction within the CIGS layer (buried junction). Several geometrical and physical parameters of the materials involved in the junction formation are critical to the cells performance. Many studies have shown that the optimum band gap of CIGS is around 1.2 eV, corresponding to an absorber Ga-content approximately equal to 0.3. The typical thickness of the absorber of high efficiency CIGS-based solar cells is in the range of 1.5 to 3  $\mu\text{m}$  [1-4]. In fact, CIGS is a direct band gap material with a high absorption coefficient ( $10^5 \text{ cm}^{-1}$ ), so that a thin thickness of 0.5  $\mu\text{m}$  is sufficient to absorb 90% of the incident photons [2][3]. As for the defect layer, the results published are often inconsistent: it has been found that the absorber surface layer is inverted to n-type and, to explain this inversion, some authors identify the layer to an n-type ODC with a large band gap [5-14]. They have observed several candidates among which  $\text{CuIn}_3\text{Se}_5$ ,  $\text{CuIn}_5\text{Se}_8$ ,  $\text{Cu}_2\text{In}_4\text{Se}_7$  and  $\text{Cu}_3\text{In}_5\text{Se}_9$ . Others claim that there is no ODC structure observed on the CIGS surface and that the surface layer inversion is due to either a large bending of the conduction band minimum toward Fermi level or a valence band maximum much lowered with respect to the Fermi level [6][15-17]. It is also indicated that the surface layer thickness is about 15 nm [18-19]. But in any case, it is established experimentally that the surface of CIGS has a wide band gap with a valence band maximum considerably below the Fermi level, while the position of conduction band minimum remains approximately constant [8]. This is the reason of n-type conductivity.

The difficulty comes from the fact that many physical properties of CIGS alloys are not yet clarified. Furthermore, different deposition techniques are used in laboratories to

prepare thin-film CIGS semi-conductor materials for photovoltaic conversion. Each technique has its own specifications, which of course leads to different parameters for obtaining a particular property. This is also frequently encountered for the same deposition method as a function of the equipment used. Thus, the material parameters can be varied within wide ranges. The physical properties of the materials can be controlled if a good control of the growth parameters such as temperature, pressure, rate of the gas flow of the constituents of the materials (Mo, Zn, Se, Cu, S, In, Ga, etc.), the deposition time and the pH was achieved. An environment where the risk of particulate contamination is very low also contributes to obtaining the reproducibility of these properties.

In a first article [20], we optimized CIGS-based solar cells by studying the parameters of the key parts of the solar cell, in particular the thickness and Ga-content of the absorber layer, thickness of the buffer layer and doping concentrations of absorber and buffer layers. We found a maximum conversion efficiency of 26%. In this article we extend our investigation to the case of electronic parameters: the buffer layer, the CIGS absorber band gap, the conduction band discontinuity; the band gap and the thickness of the defect layer between the absorber and buffer. The buffer layer acts as a window layer, so it should be very thin and have a band gap higher than that of the absorber, to allow the absorption of almost all of the radiation in the absorber. The conduction band discontinuity affects the interface recombination. Finally, the band gap and the thickness of the defect layer between the absorber and buffer which play an important role in the solar cells performance.

In this work, we used AFORS-HET software to carry out numerical simulation of thin-film solar cells based on CIGS with ZnS as an alternative buffer material to CdS. We investigate the effects of the band gaps of the key materials (ZnS, CIGS), band gap and thickness of the defect layer, as

Volume 6 Issue 11, November 2017

[www.ijer.net](http://www.ijer.net)

Licensed Under Creative Commons Attribution CC BY

well as the conduction band offset of buffer/absorber layers on the photovoltaic parameters ( $J_{SC}$ ,  $V_{OC}$ ,  $FF$  and  $\eta$ ). Since the processing technology of CIGS-based solar cells has not yet reached a maturity similar to that of silicon solar cells, the aim of this work is to examine the trend in the solar cell performance when the critical electrical properties of the involved key materials are varied.

## 2. Device Numerical Modeling and Simulation

We have considered a CIGS-based solar cell whose energy-band diagram is schematically illustrated in figure.1. It consists of seven stacked layers including top and back contacts. These contacts are assumed as ohmic with surface recombination velocity  $S_n = S_p = 10^7 \text{cm/s}$ . The model presented here is based on the Fermi level pinning which is modelled by a high density:  $3 \cdot 10^{18} \text{cm}^{-3}$ , of donor defects located at 0,2 eV below the CIGS absorber conduction band. These have a small electron and hole capture cross-section,  $\sigma_n = \sigma_p = 10^{-18} \text{cm}^2$ , to separate pinning defects from recombination within the defect layer. In the simulations, two Gaussian distributions of deep defects with narrow

bandwidths are considered: deep donor defects are assigned to the p-type materials and deep acceptor defects to the n-type materials. The bulk recombination defect states are positioned at the mid-gap of the respective layers and the interface defects are positioned at the mid-gap of the lowest band gap of the two adjacent materials.

Using Shockley-Read-Hall recombination model, the simulator solved the fundamental one-dimensional equations (Poisson's equation and the transport and continuity equations for electrons and holes) under steady-state conditions and calculated the internal characteristics, such as band diagram, generation and recombination rates, carrier densities and cell currents. The cell is subjected to AM.1,5G solar spectrum with an incident power density of  $100 \text{mW/cm}^2$  at room temperature. The effects of series resistance and shunt resistance are not taken into account. The input parameters for each kind of material are listed in table 1. All parameters of the key materials, except the band gaps and electron affinities, are kept constant. In the same way, the band gap and the thickness of the defect layer are variable.

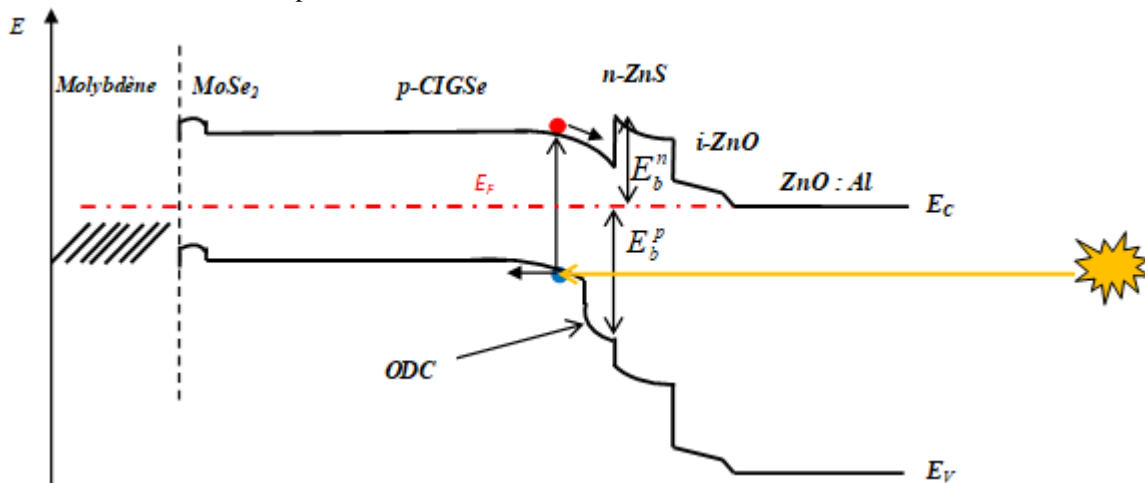


**Figure 1:** Energy band diagram of the ZnS/CIGS solar cell under equilibrium condition

**Table 1:** Input parameters used for the solar cell simulation. (a) and (d) denote shallow acceptor and donor while (A) and (D) denote deep acceptor and donor

Layers properties					
	CIGSe	ODC	ZnS	i-ZnO	ZnO :Al
Thickness( $\mu\text{m}$ )	3	variable	0,03	0,02	0,03
Band gap $E_g$ (eV)	variable	variable	variable	3,2	3,2
Electron affinity $\chi$ (eV)	4,5 [10]	4,5 [10]	variable	4,5 [10]	4,5 [10]
Dielectric constant $\epsilon_r$	13,6 [7][10]	13,6 [7][10]	9	9 [7][10]	9 [7][10]
$N_C$ ( $\text{cm}^{-3}$ ) / $N_V$ ( $\text{cm}^{-3}$ )	$6,8 \cdot 10^{17}$ / $1,5 \cdot 10^{19}$ [7][10]	$6,8 \cdot 10^{17}$ / $1,5 \cdot 10^{19}$ [7][10]	$2,2 \cdot 10^{18}$ / $1,8 \cdot 10^{19}$	$3 \cdot 10^{18}$ / $1,7 \cdot 10^{19}$ [7][10]	$3 \cdot 10^{18}$ / $1,7 \cdot 10^{19}$ [7][10]
$S_{th}^p, S_{th}^n$ (cm/s)	$10^7$				
$\mu_n$ ( $\text{cm}^2/\text{Vs}$ ) / $\mu_p$ ( $\text{cm}^2/\text{Vs}$ )	100 / 50 [7] [10]	10 / 1.25 [7] [10]	100 / 25	100 / 31 [7]	100 / 31 [7] [10]
Doping level ( $\text{cm}^{-3}$ )	$5 \cdot 10^{17}$ (a)	$5 \cdot 10^{17}$ (a)	$10^{18}$ (d)	$10^{18}$ (d)	$10^{20}$ (d)
Bulk Gaussian defect states					
Nt ( $\text{cm}^{-3}$ )	$10^{14}$ (D) [7][9][10]	$10^{14}$ (D) [7][9][10]	$10^{17}$ (A)	$10^{17}$ (A)	$10^{17}$ (A)

$E_{GD}, E_{GA}$ (eV)	<b>Mid-gap</b>				
$W_{GD}, W_{DA}$ (eV)	0.01				
$\sigma_n$ (cm <sup>2</sup> )/ $\sigma_p$ (cm <sup>2</sup> )	$10^{-13}/$ $10^{-15}$ [7][10]	$10^{-13}/$ $10^{-15}$ [7][10]	$10^{-15}/ 5.10^{-13}$ [7][10]	$10^{-15}/$ $5.10^{-13}$ [7][10]	$10^{-15}/$ $5.10^{-13}$ [7] [10]
<b>Interface Gaussian defect states</b>					
	<i>CIGSe/ODC</i>	<i>ODC(CIGSe)/ZnS</i>	<i>ZnS/i-ZnO</i>		
$\Delta E_C$ (eV)	0	0.35 (0.35)	-0.35		
$\Delta E_V$ (eV)	-0.15	-1.91 (-2.06)	0,05		
Nt (cm <sup>-2</sup> )	$10^{10}$ (D)	$3.10^{18}$ (D)	-		
$E_{GD}/E_{GA}$ (eV)	<b>Mid-gap</b>				
$W_{GD}/W_{DA}$ (eV)	0.01				
$\sigma_n$ (cm <sup>2</sup> )/	$10^{-13}$	$10^{-13}$	- [7] [10]		
$\sigma_p$ (cm <sup>2</sup> )	$10^{-15}$	$10^{-15}$			

### 3. Results and Discussion

#### 3.1 Effects of band gaps of the absorber and buffer layers

In the studied hetero-structure, it is generally argued that the buffer layer participates in the p-n junction formation, but its actual role is always controversial, since the p-n junction is buried in the chalcopyrite material. The solar cell absorber layer is the only part where photo-generation of electron-hole pairs occurs. Under these conditions, the buffer layer should act as a window that transmits most of the solar radiation and the band gap is the parameter that really enables to modify its sunlight absorption. We have noticed that the measured and published values in the literature about the band gaps of ZnS and CIGS are in the ranges 3.5-3.84 eV and 1.16-1.2 eV for  $x = 0.3$ , respectively [21-29]. As explained above, the variations of these values are due to

variations of the material properties elaborated using different deposition techniques. In this section, we have investigated the cell performance as function of the ZnS and CIGS materials band gap. Varying the buffer layer band gap in the range of 3 to 4 eV and the absorber layer band gap in the range of 1 to 1.2 eV, we observe no effect on the efficiency. On the other hand, the solar cell characteristic parameters are very sensitive to the CIGS band gap variation (figure.2). The conversion efficiency ( $\eta$ ) increases significantly with the absorber band gap: from 21% to 26%, for a band gap of 1.2 eV. We observe the same for open circuit voltage ( $V_{OC}$ ): from 650 to 850 mV, and fill factor (FF): from 82.5% to 85.5%. The increase of these parameters with the band gap is almost linear. The short circuit current ( $J_{SC}$ ) decreases: from 40 to 36.5 mA/cm<sup>2</sup>, the amount of absorbed photons in CIGS layer decreasing with the band gap.

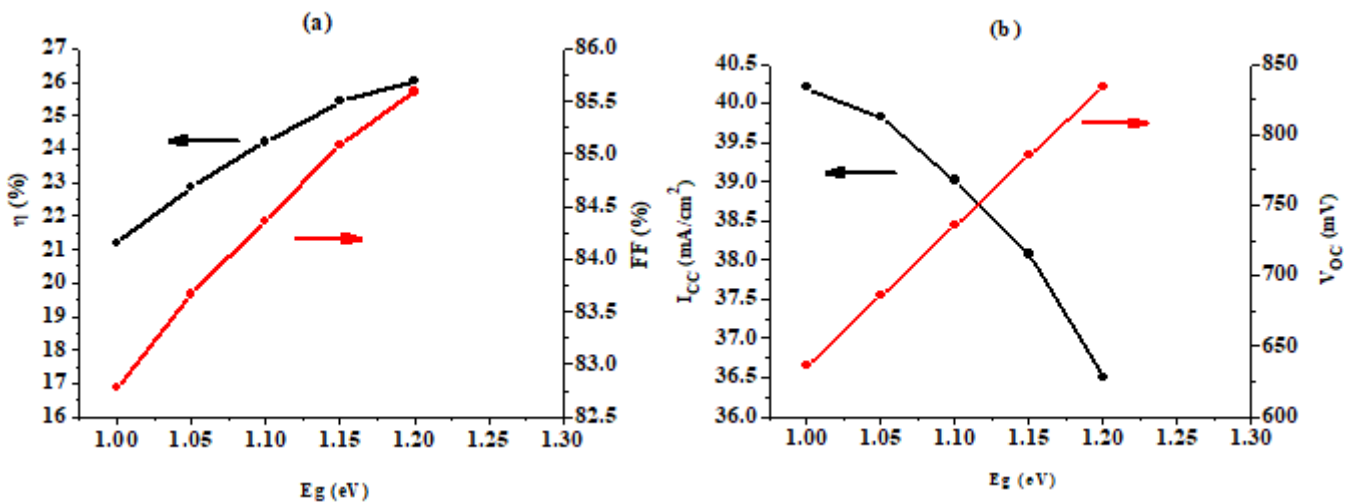


**Figure 2:** The solar cell performance as a function of CIGS band gap

#### 3.2 Effect of the interface conduction band offset

The conduction band offset  $\Delta E_C$  is one of the most important parameters that affects the performance of hetero-junction solar cells based on CIGS [30-33]. Several authors clearly explained the influence of the conduction band offset, in both cases whether positive (spike) or negative (cliff). They showed that a spike (figure 3(a)) acts as a barrier against photo-generated electrons in the CIGS absorber layer while

a cliff (figure 3(b)) acts as a barrier against electrons injected from the buffer layer [34-36].

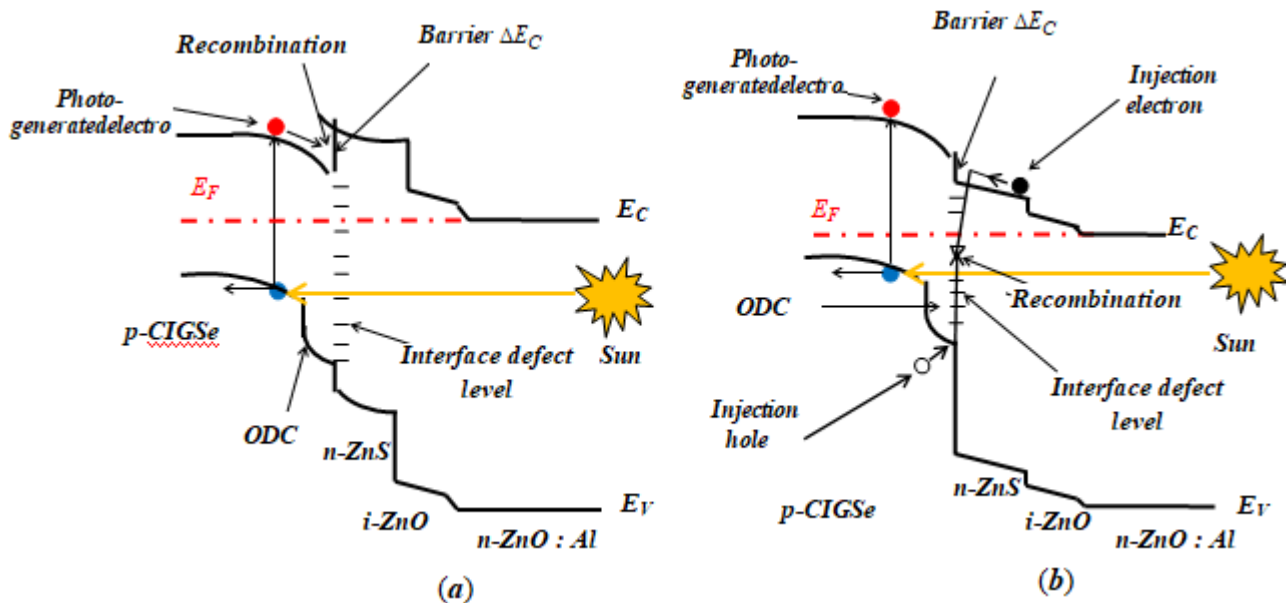


Figure 3: Schematics band diagram of the cell structure when (a) a spike or (b) a cliff is formed

In this part of our work the band gap of the ZnS window was assumed to be a constant equal to 3.6 eV and the conduction band offset at buffer/absorber interface was varied by changing the electron affinity of ZnS layer. Figure.4 shows the effect of conduction band discontinuity on the solar cell characteristic parameters. As it can be seen in this figure, the short circuit current decreases slightly when a spike is formed. This is caused by the photo-generated electrons being blocked and unable to cross over the barrier. When a cliff is formed, there is no barrier against photo-generated

electrons. However, the cliff causes recombination between the majority electrons injected from the buffer layer and the interface defects, which alters the open circuit voltage and the fill factor while the short circuit current is almost constant. The fill factor decreases when a high spike or a deep cliff is formed. The optimum value of the conduction band offset at the interface between buffer and absorber layers is of 0.3 eV where an efficiency of 26% is reached. Moreover, in the range of 0.1 to 0.35 eV the solar cell efficiency is nearly constant.

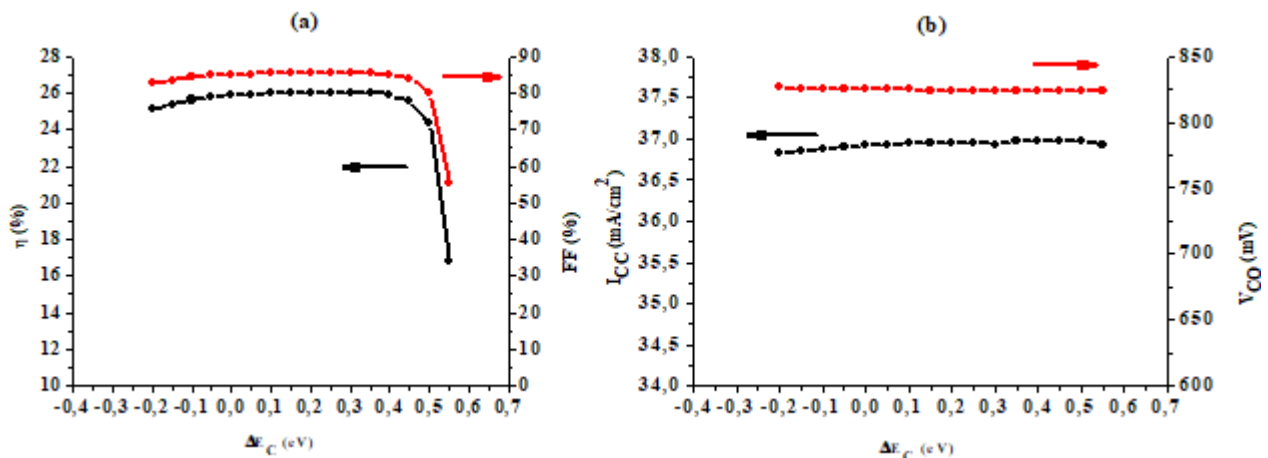


Figure 4: The solar cell performance as a function of the conduction band offset of buffer- absorber layers

### 3.3 Effects of defect layer band gap and thickness

All work on the CIGS thin-film agree that the surface material has a wide band gap which partly explains the high performance of solar cells based on this material [7-15]. Using the Fermi level pinning model, the defect layer parameters are chosen similar to that of the bulk CIGS, except the band gap, the thickness and the carrier mobilities. Under these conditions, figure.5 displays the effect of the defect layer band gap on the cell performance. As can be seen  $V_{OC}$  and  $FF$  increase rapidly with the band gap up to a value of  $E_g = 1.25$  eV where a maximum conversion efficiency of 26% is reached. This trend is explained by the

fact that the barrier  $E_b^p$  increases. There by the recombination at ZnS/CIGS interface decreases. Above  $E_g = 1.25$  eV,  $V_{OC}$  and  $FF$  are almost constant while  $J_{SC}$  decreases slightly because the contribution of the thin surface layer in the carriers photo-generation decreases with the band gap increase.

We have also investigated the effect of the defect layer thickness on the solar cell characteristic parameters. In the literature some authors argue that the defect layer is formed by 1 or 2 atomic layers while others claim that it is several nanometers thick (up to 60 nm)[6][9][16][18-19]. In the following, the defect layer thickness was varied from 1 to 31

nm. The influence of the defect layer thickness on the open circuit voltage is negligible because of the high band gap of the ZnS layer toward the interface. Similarly, the short circuit current decreases almost linearly with a very low slope of 0.013 mA/cm<sup>2</sup>/nm. This decrease of  $J_{SC}$  is due to the low carrier mobilities, which enhances the bulk

recombination. The fill factor remains almost constant up to a thickness of about 15nm and decreases slightly when the thickness of defect layer exceeds this value. Consequently, the cell conversion efficiency follows the fill factor trend.

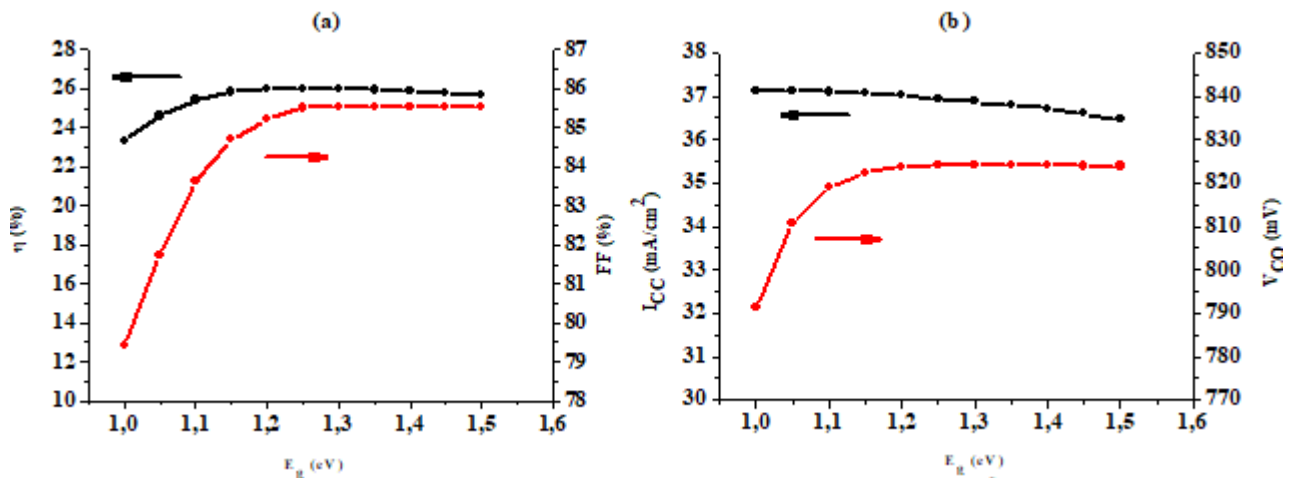


**Figure 5:** The solar cell performance as a function defect layer band gap

#### 4. Conclusion

The present work has focused on the examination of the effects of the band gaps of the materials forming the n-ZnS/p-CIGS hetero-junction. The effects of the band gap and thickness of the defect layer present between the two adjacent materials has also been investigated. Calculations have been performed using the AFORS-HET simulator. The results show that the solar cell performance is more sensitive to the electrical properties of the absorber and defect layers and is particularly influenced by the defect layer thickness. The band gap of ZnS has no significant effect on the characteristic parameters of the solar cell while the band gap of the CIGS absorber layer and that of the defect layer are more critical. Indeed, an increase of these band gaps enhances the solar cell efficiency. But; above 1.25 eV, the band gap of the defect layer alters the cell efficiency. The defect layer thickness can reach up to 15 nm without altering the solar cell optimum efficiency, which is of 26%. As for the effect of the conduction band offset, the simulation results show that a spike in the range of 0.1 to 0.35 eV is very advantageous and that the solar cell efficiency remains almost constant within this range. The optimum height of the spike is of 0.3 eV above the conduction band of the CIGS absorber.

#### References

- [1] N. Amin, Michael Tang and Kamaruzzaman Sopian. "Numerical Modeling of the Copper-Indium-Selenium (CIS) based Solar Cell Performance by AMPS-1D". The 5th Student Conference on Research and Development-SCORED 2007 11-12 December 2007, Malaysia.
- [2] N. Touafek, R. Mahamdi. "Back Surface Recombination Effect on the Ultra-Thin CIGS Solar Cells by SCAPS". International Journal of Renewable Energy Research N.Touafek et al., Vol.4, No.4, (2014).
- [3] N. Touafek, R. Mahamdi. "Impact of [Ga]/[In+Ga] Ratio on the Generation-Recombination Rates of Cu(In,Ga)Se<sub>2</sub> Solar Cells". 2ème conférence Internationale des énergies renouvelables CIER-(2014) Proceedings of Engineering and Technology – PET
- [4] N. Amin, P. Chelvanathan, M. I. Hossain and K. Sopian. Numerical modelling of ultra-thin Cu(In,Ga)Se<sub>2</sub> solar cells. Energy Procedia 15 (2012) 291-298.
- [5] C-H Huang. "Effects of junction parameters on Cu(In,Ga)Se<sub>2</sub> solar cells". Journal of Physics and Chemistry of Solids 69 (2008) 779–783.
- [6] D. Liao and A. Rockett. "Cu depletion at the CuInSe<sub>2</sub> surface". Applied Physics Letters, Vol.82, Number 17 (2003).
- [7] S. B. Zhang, Su-Huai Wei, A. Zunger, and H. K. Yoshida. "Defect physics of the CuInSe<sub>2</sub> chalcopyrite semiconductor". Physical Review B Vol. 57, Number 16 (1998).
- [8] D. Schmid, M. Ruckh, F. Grunwald and H.W. Schock, "Chalcopyrite/defect chalcopyrite heterojunctions on the basis of CuInSe<sub>2</sub>", Journal of Applied Physics, Vol. 73 (6), 1993, pp. 2902.
- [9] D. Schmid, M. Ruckh, H. Werner Schock. "A comprehensive characterization of the interfaces in Mo/CIS/CdS/ZnO solar cell structures". Solar Energy Material and solar cells 41/42 (1996) 281-294.
- [10] Z. Li, M. Nishijima, A. Yamada, and M. Konagai. "Growth of Cu(In,Ga)Se<sub>2</sub> thin films using ionization Ga source and application for solar cells". Phys. Status Solidi C 6, N<sup>o</sup>. 5, 1273–1277 (2009).
- [11] A. Zunger, S. B. Zhang and S-H Wei. "Revisiting The Defect Physics in CuInSe<sub>2</sub> and CuGaSe<sub>2</sub>", in Proceedings of the 26th IEEE PV specialist conf., edited by P. A. Basore, (AIP, New York, 1998), p. 313.
- [12] S. Levchenko, L. Durán, G. Gurieva, M. I. Alonso, E. Arushanov, C. A. Durante Rincón, and M. León. "Optical constants of Cu(In<sub>1-x</sub>Ga<sub>x</sub>)<sub>5</sub>Se<sub>8</sub> crystals". Journal of Applied Physics 107, 033502 (2010).

- [13] H. Zhao, M. Kumar, and C. Persson. "Density functional theory study of ordered defect Cu-(In,Ga)-Se compounds". *P hys. Status Solidi C* 9, No. 7, 1600–1603 (2012) / DOI 10.1002/pssc.201100671.
- [14] S.H. Kwon, S.C. Park, B. T. Ahn, K. H. Yoon and J. Song. "Effect of CuIn<sub>3</sub>Se<sub>5</sub> Layer Thickness on CuInSe<sub>2</sub> Thin Films and Devices". *Solar Energy* Vol. 64, Nos 1-3, pp. 55–60, 1998.
- [15] Y. Yan, K. M. Jones, J. Abushama, M. Young, S. Asher, M.M. Al-Jassim, and R. Noufi, "Microstructure of surface layers in Cu(In,Ga)Se<sub>2</sub> thin films", *Applied Physics Letters*, Vol.81, 2002, pp.1008.
- [16] R. Herberholz, U. Rau, H. W. Schock, T. Haalboom, T. Gödecke, F. Ernst, C. Beilharz, K. W. Benz and D. Cahen, "Phase segregation, Cu migration and junction formation in Cu(In, Ga)Se<sub>2</sub>", *Eur. Phys. J. AP*, Vol. 6, 1999, pp.131.
- [17] U. Rau, D. Braunger, R. Herberholz, H. W. Schock, J.-F. Guillemoles and L. Kronik and D. Cahen. "Oxygenation and air-annealing effects on the electronic properties of Cu.(In,Ga)Se<sub>2</sub> films and devices". *Journal of Applied Physics* Vol. 86, Number 1 (1999).
- [18] I M Dharmadasa. "Fermi level pinning and effects on CuInGaSe<sub>2</sub>-based thin-film solar cells". *Semicond. Sci. Technol.* 24 (2009) 055016 (10pp).
- [19] I.M. Kotschau, H.W. Schock. "Depth profile of the lattice constant of the Cu-poor surface layer in (Cu<sub>2</sub>Se)<sub>1-x</sub>(In<sub>2</sub>Se<sub>3</sub>)<sub>x</sub> evidenced by grazing incidence X-ray diffraction". *Journal of Physics and Chemistry of Solids* 64 (2003) 1559–1563.
- [20] A. Sylla, S. Touré, J-P Vilcot. "Numerical Modeling and Simulation of CIGS-Based Solar Cells with ZnS Buffer Layer". *Scientific Research Publishing. Open Journal of Modelling and Simulation*, 2017, 5, 218-231
- [21] M.Y. Nadeem, W. Ahamed. "Optical Properties of ZnS Thin Films". *Turk J Phy* 24 (2000), 651-659
- [22] T. Nakada, K. Furumi, and A. Kunioka. "High-Efficiency Cadmium-Free Cu(In,Ga)Se Thin-Film Solar Cells with Chemically Deposited ZnS Buffer Layers". *IEEE Transactions on Electron Devices*, Vol. 46, N<sup>o</sup>. 10, (1999).
- [23] D. Kurbatov, A. Opanasyuk, S. Kshnyakina, V. Melnik, V. Nesprava. "Luminescent and Optical Characteristics of Zinc Sulfide Thin Films Produced by Close-Spaced Vacuum Sublimation". *Rom. Journ. Phys.*, Vol. 55, Nos. 1–2, P. 213–219, (2010).
- [24] Y. He, L. Zhang, L. Wang, M. Li, X. Shang, X. Liu, Y. Lu, B. K. Meyer. "Structural and optical properties of single-phase ZnO<sub>1-x</sub>S<sub>x</sub> alloy films epitaxially grown by pulsed laser deposition". *Journal of Alloys and Compounds* 587 (2014) 369–373.
- [25] T. Dullweber, U. Rau, M.A. Contreras, R. Noufi, and H.-W. Schock. "Photogeneration and Carrier Recombination in Graded Gap Cu(In,Ga)Se<sub>2</sub> Solar Cells". *IEEE Transactions on Electron Devices*, Vol. 47, N<sup>o</sup>. 12, (2000).
- [26] S-H Wei, S. B. Zhang, and A. Zunger. "Effects of Ga addition to CuInSe<sub>2</sub> on its electronic, structural, and defect Properties". *Applied Physics Letters* Vol. 72, N<sup>o</sup> 24 (1998).
- [27] D.S. Albin, J.R. Tuttle, G.D. Mooney, J.J. Carapella, A. Duda, A. Mason, and R. Noufi. "A Study on the optical and microstructural characteristics of quaternary Cu(In,Ga)Se<sub>2</sub> Polycrystalline thin films". *Photovoltaic Specialists Conference*, 1990. *Conference Record of the Twenty First IEEE*.
- [28] A. Rockett. "Performance-limitations in Cu(In,Ga)Se<sub>2</sub>-based heterojunction solar cells". *Photovoltaic Specialists Conference, 2002. Conference Record of the Twenty-Ninth IEEE*.
- [29] S.-Y Kuo, M.-Y. Hsieh, D.-H. Hsieh, H.-C. Kuo, C.-H. Chen, and F.-I Lai. "Device Modeling of the Performance of Cu(In,Ga)Se<sub>2</sub> Solar Cells with V-Shaped Bandgap Profiles". *International Journal of Photoenergy* Volume 2014, Article ID 186579, 6 pages. (Published 14 July 2014)
- [30] N. Khoshsirat and N. A. Md. Yunus. "Copper-Indium-Gallium diSelenide (CIGS) Nanocrystalline Bulk Semiconductor as the Absorber Layer and Its Current Technological Trend and Optimization". *Nanoelectronics and Materials Development*. <http://dx.doi.org/10.5772/64166>.
- [31] T. Minemoto, Y. Hashimoto, W. Shams-Kolahi, T. Satoh, T. Negami, H. Takakura, Y. Hamakawa. "Control of conduction band offset in wide-gap Cu(In,Ga)Se<sub>2</sub> solar cells". *Solar Energy Materials & Solar Cells* 75 (2003) 121–126
- [32] M. Gloeckler, J.R. Sites. "Efficiency limitations for wide-band-gap chalcopyrite solar cells". *Thin Solid Films* 480–481 (2005) 241–245.
- [33] T. Minemoto, T. Matsui, H. Takakura, Y. Hamakawa, T. Negami, Y. Hashimoto, T. Uenoyama, M. Kitagawa. "Theoretical analysis of the effect of conduction band offset of window/CIS layers on performance of CIS solar cells using device simulation". *Sol. Ene. Mat. & Sol. Cells* 67, 83-88 (2001).
- [34] T. Minemoto, T. Matsui, H. Takakura, Y. Hamakawa, T. Negami, Y. Hashimoto, T. Uenoyama, M. Kitagawa. "Theoretical analysis of the effect of conduction band offset of window/CIS layers on performance of CIS solar cells using device simulation". *Sol. Ene. Mat. & Sol. Cells* 67, 83-88 (2001).
- [35] S. Sharbati and J.R. Sites. "Impact of the band offset for n-Zn(O, S)/p-Cu(In,Ga)Se<sub>2</sub> Solar cells". *IEEE Journal of Photovoltaics*. Vol. 4 N<sup>o</sup> 2. (2014)
- [36] M. Gloeckler, J.R. Sites. "Efficiency limitations for wide-band-gap chalcopyrite solar cells". *Thin Solid Films* 480–481 (2005) 241–245.